

10p

X 63-11443
Code sd
NASA TT F-8361

ELECTRIC BREAKDOWN OF MICROGAPS IN A GAS

by U. Frolov

FACILITY FORM 602	N 71-71410	
	(ACCESSION NUMBER)	(THRU)
	10 (PAGES)	None (CODE)
	(NASA CR OR TMX OR AD NUMBER)	(CATEGORY)

NATIONAL AERONAUTICS AND SPACE ADMINISTRATION
WASHINGTON
February 1963

Y 140 Y 903 3 1963

ELECTRIC BREAKDOWN OF MICROGAPS IN A GAS

Engineer A. I. Frolov, Ufa

A knowledge of the mechanism of electric breakdown in microgaps (i.e., gaps measuring microns and tens of microns) is essential for the understanding of the physical phenomena that occur in the opening contacts of relays, vibrator converters, induction coils, the brush contacts of electrical machinery, and in sliding contacts in general. Breakdown of this kind is also interesting because it is there that surface phenomena on electrodes come into play and impart a special character to the behavior of microgaps in electric fields. The dielectric strength of the microgap is found to depend not only on the composition and density of the medium or on the distance between electrodes, but to a considerable degree also on the properties of the electrode material.

It is assumed in the prevalent opinions regarding microgap breakdown [1 and 2] that the gap breaks down in region OB (Fig. 1) at a potential lower than the minimum sparking potential for the given medium, and that electric field intensity causing the gap breakdown remains constant. The main physical processes are field emission, which causes the anode to heat up, and the extraction of the metal by the electrostatic forces, which leads to the formation of minute metal bridges between the electrodes.

In region BC, an avalanche-like discharge occurs. For the avalanche to be formed, it is necessary to have a certain minimum distance, or more accurately a minimum number of mean free paths of the elementary particles between collisions, and consequently discharge between the closest points on the electrode surfaces is more difficult to effect than discharge between more remote points. Thus, in the region BC the discharge follows the most favored path δ_{\min} (amounting to 6×10^{-4} cm for air at atmospheric pressure), which remains constant within this region. As a result the discharge-firing potential remains also constant.

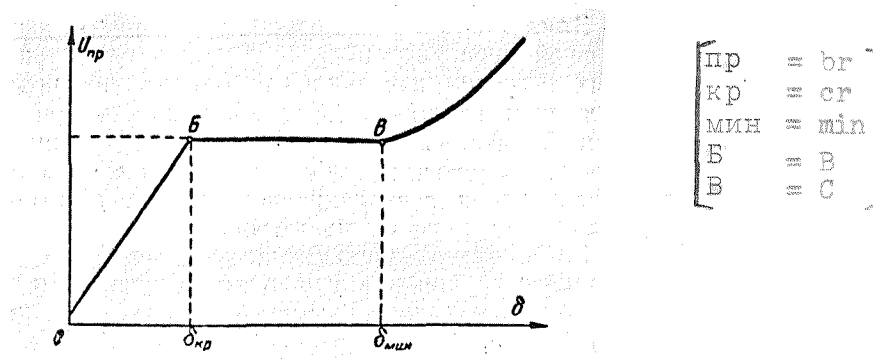


Fig. 1. The potential needed to restore the contact or create a spark breakdown as a function of the distance between the nearest point of the electrode (from the data of [1 and 2]).

Beyond the point $\delta = \delta_{min}$, the distance between the nearest points on the contact surfaces becomes greater than the minimum distance necessary for the formation of the electron avalanche; in this region the dependence of the breakdown potential on the distance should be governed by the customary laws.

We used the following procedure to investigate the dielectric-strength characteristics of microgaps. Freshly cleaned and thoroughly polished contacts were opened at a constant speed (within the limits of the investigated distances, i.e., on the order of 0.1 mm) by means of a cam mechanism. Cyclic operation with 8 -- 10 "close -- open" cycles per second was employed. In all the experiments reported below, the contacts moved apart at a speed of 10 cm/sec. The contact pressure in the closed state was 25 -- 30 grams.

At the instant when the contacts started to move apart, a special fixture triggered the driven sweep of an oscilloscope, as well as a gating circuit, which generated, after a specified time delay, a single voltage pulse in the form of a sinusoidal half-wave with a base 6 -- 8 sec. The amplitude of this half-wave could be adjusted between 0 and 1,000 V; the time of occurrence of this half-wave, referred to the instant when the contacts broke, was also adjustable.

By smoothly increasing the amplitude of the half-wave, it was easy to observe on the oscilloscope screen the instant when the gap breakdown occurred between the separating contacts. From the known speed it was possible to determine the distance between the nearest points of the contact surface at the given instant of time, by counting the time markers from the start of contact separation.

The circuitry for the pulse generator, the synchronization of the start of contact separation, the triggering of the generator, and the triggering of the driven sweep are shown in Fig. 2.

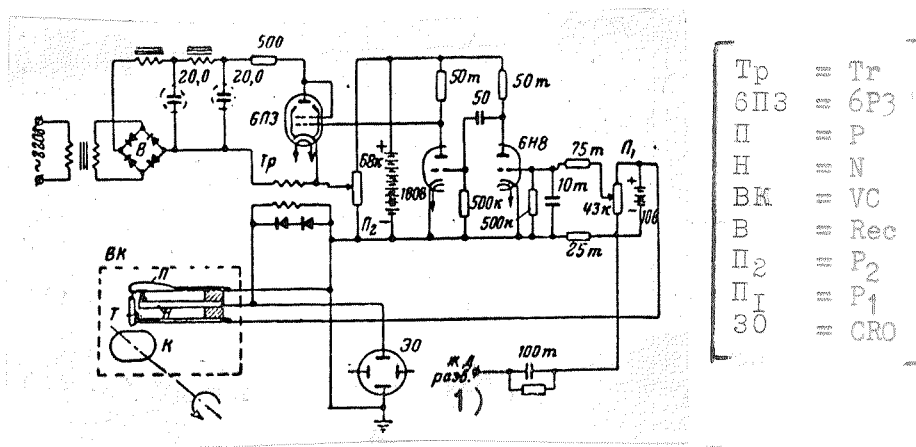


Fig. 2. Diagram of test setup.

P -- moving contact located on a specially shaped spring; N -- stationary contact; T -- plunger; K -- specially shaped cam; VC -- vacuum chamber; Rec -- rectifier; CRO -- cathode ray oscillograph; Tr -- transformer.

1) Driven sweep.

The voltage pulse was produced on the contacts by transferring the energy accumulated in the primary winding of the step-up transformer to the secondary circuit at the instant when the output tube was cut off. The pulse delay time relative to the start of contact separation was set with the aid of potentiometer P_1 , while the height of the pulse was regulated by varying the current in the transformer primary with the aid of potentiometer P_2 . The duration (width) of the pulse was regulated by changing the air gap of the transformer and the number of turns in its windings.

The aforementioned three processes were synchronized mechanically, as shown in Fig. 2, by using a specially designed vibrator. The pulse amplitude was measured by placing a suitably calibrated grid on the oscilloscope screen.

Fig. 3 shows the waveform of the pulse on the contacts prior to and at the instant of gap breakdown.

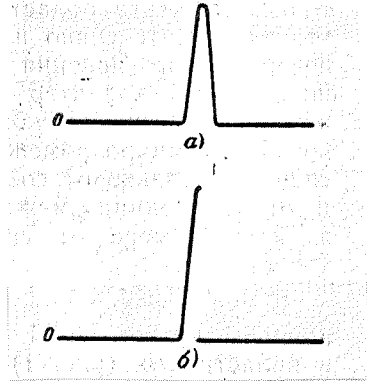


Fig. 3. Waveform of contact voltage pulse. The point 0 corresponds to the start of contact separation.

a) prior to breakdown; b) at the instant of breakdown.

The method employed eliminated the flow of current at the instant of contact separation, and consequently the formation of metallic bridges, microarcs, and the accompanying damage to the polish of the contact surface.

The characteristics of the dielectric strength of the microgaps were determined for contact pairs made of the following metals: nickel, silver, an alloy of 75% platinum and 25% iridium, iron, aluminum, and copper. The insulating medium was in all cases atmospheric air at pressures ranging from 5 mm. Hg. to normal. The results of the experiments are illustrated in Figs. 4 and 5.

If we start from the theory of avalanche breakdown in the region BC (Fig. 1), it is obvious that the position of the point C should be determined by the Paschen law, i.e., the point C should shift with decreasing pressure to the right, towards the larger values of the distance (the product $p\delta_{\min}$ should remain constant).

However, the microgap dielectric-strength characteristics which we plotted do not confirm this fully natural consequence of the foregoing microgap breakdown theory. The position of the point C depends very little on the pressure of the surrounding medium, and with decreasing pressure this point shifts towards smaller δ . Furthermore, the position of the point C (the point of inflection of the dielectric-strength curve where the horizontal portion begins to rise) is a characteristic of the contact-pair material; the value of δ_{\min} amounts in this case to $(6 -- 15) \times 10^{-4}$ cm at normal atmospheric pressure (silver and iron give the lowest and highest values, respectively). There is no sharp transition whatever between the regions OB and BC, nor is the breakdown voltage strictly constant in region BC (one is more likely to note a tendency towards a more or less smooth rise of the breakdown potential in the region BC).

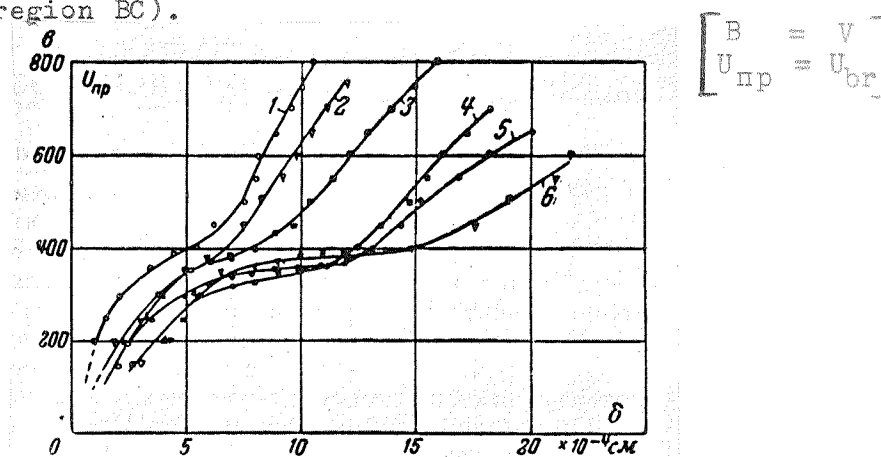


Fig. 4. Dependence of the breakdown voltage on the distance between the nearest points of the electrodes, δ , under normal atmospheric pressure.

1 -- silver; 2 -- platinum-iridium-25 alloy; 3 -- copper;
4 -- aluminum; 5 -- nickel; 6 -- iron.

The dependence of the breakdown potential on the distance (Fig. 4) in the region OBC is more reminiscent of the potential distribution in the cathode drop region of a glow discharge, since the approximate condition [3],

$$U_B = \frac{1}{2} E \delta_{\min} \quad [\min = \min] \quad (1)$$

holds true in approximately all cases.

Here U_B corresponds to the normal cathode potential drop in the glow discharge;

δ_{\min} -- length of the region of the glow-discharge cathode drop;

E_0 -- field intensity at the cathode surface. The corresponding values are listed in the table.

Relation (1) is equivalent to assuming the presence of a resultant positive space charge of more or less constant density near the cathode at the instant immediately preceding the breakdown. Integrating the Poisson equation

$$\frac{dE}{d\delta} = -4\pi\rho \quad (\rho = \text{const}) \quad (2)$$

under the following initial conditions

$$\delta = 0; E = E_0; U = 0,$$

we obtain

$$E = E_0 - 4\pi\rho\delta \quad (3)$$

and

$$U = E_0\delta - 4\pi\rho \frac{\delta^2}{2}. \quad (4)$$

Characteristics of the dielectric strength of microgaps at normal atmospheric pressure.

Contact material	Field intensity at the cathode surface, $E_0 = \text{V/cm}$	Distance to a point of inflection, $\delta_{\min}, \text{ cm}$	Breakdown potential U_B at the point δ_{\min} , volts	calculated value of $\delta_{\min}, = 2U_B/E_0, \text{ cm}$
Silver	$1.8 \cdot 10^6$	$6 \cdot 10^{-4}$	425	$4.7 \cdot 10^{-4}$
Platinum-iridium	$0.90 \cdot 10^6$	$6.5 \cdot 10^{-4}$	390	$8.7 \cdot 10^{-4}$
Copper	$0.80 \cdot 10^6$	$8.5 \cdot 10^{-4}$	415	$10.4 \cdot 10^{-4}$
Aluminum	$0.53 \cdot 10^6$	$11.5 \cdot 10^{-4}$	370	$14.0 \cdot 10^{-4}$
Nickel	$0.77 \cdot 10^6$	$12 \cdot 10^{-4}$	370	$9.6 \cdot 10^{-4}$
Iron	$0.53 \cdot 10^6$	$15 \cdot 10^{-4}$	400	$15 \cdot 10^{-4}$

Assuming that when $\delta = \delta_{\min}$ the field intensity at the anode vanishes, we have $4\pi\rho = E_0/\delta_{\min}$:

$$U_B = \frac{1}{2} E_0 \delta_{\min}. \quad [\text{mm} = \text{min}] \quad (5)$$

We can thus assume that the microgap is appreciably ionized at the instant prior to the discharge; in this case the resultant effect of the external field and of the space-charge field leads to the creation of an approximately constant field intensity at the cathode (with a value different for each electrode material).

But it follows in such a case that the microgap breakdown in the region OBC (Fig. 1) is connected with the further increase in ionization due to the sharp increase in the emission efficiency when the resultant electric field at the cathode surface reaches a value on the order of 10^6 V/cm. This value of intensity, together with the fact that the breakdown voltage does not follow the Paschen law, indicates that the basic process causing the electrons to leave is field emission; this is in contrast with glow discharge, where the main process on the cathode is secondary electron emission produced by impact of the positively charged particles against the cathode surface (a process dependent on the mean free path of the particles, i.e., connected with the product $p\delta$).

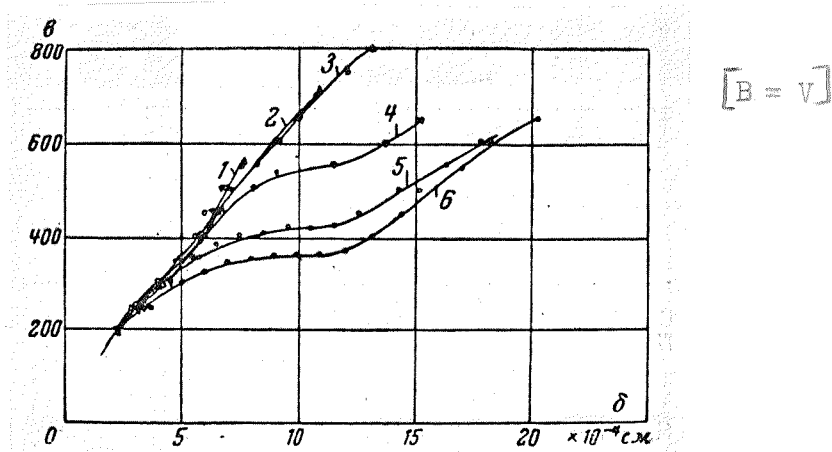


Fig. 5. Dependence of the breakdown potential on the distance between the nearest points of the electrodes, δ , for nickel electrodes. Pressure: 1 -- 10, 2 -- 60, 3 -- 140, 4 -- 300, 6 -- 450, 6 -- 760 mm Hg.

The ionization build-up, which begins after the electric field produced by the applied potential and by the intensified space charge reaches the values given above, occurs in avalanche fashion, so that conditions are created sufficient for a complete discharge of the energy accumulated in the inter-electrode capacitance and in the wiring capacitance.

A factor contributing to the pre-discharge ionization is the same field emission; as an electron source, the field emission comes into play at a field intensity on the order of 300,000 V/cm and brings about the normal course of the process [4].

The breakdown-potential characteristics shift to the left and upward with decreasing pressure because the ionization efficiency decreases, whereupon the region BC becomes shorter and even disappears completely.

As regards the behavior of the microgaps in the region beyond the point C, it seems to us that in this region the accumulation of space charges also plays a definite role.

Comparing the behavior of the breakdown potential for electrodes made of different materials (Fig. 4) and leaving aside such technical characteristics as the corrosion and erosion resistance, the tendency towards arc formation, etc., we can understand why silver, the platinum-iridium alloy, and platinum are the preferred material for low and medium-power contacts.

As follows from the curves presented, switching over-voltages occurring after the circuit is broken have a considerably lower probability of producing a spark-gap breakdown between the separating contacts.

BIBLIOGRAPHY

1. E. M. Sinel'nikov, K voprosu o kommutatsii mashin postoyannogo toka [Concerning commutation of DC machinery], *Elektrichestvo*, 1952, No. 5.
2. D. L. Pearson, Obrazovaniye metallicheskih mostikov mezhdu razvedennymi kontaktami [Formation of metallic bridges between separating contacts], *Phys. Rev.*, 1939, v. 56, p. 471.
3. L. B. Loeb, Osnovnye protsessy elektricheskikh razryadov v gazakh [Fundamental processes of electrical discharge in Gases], Gostekhizdat, 1950. [Wiley, New York, 1939].

4. M. A. Razmukhin, Povysheniye erozionnoy ustoychivosti kontaktov na malye toki v avtomaticheskikh ustroystvakh [The increase of erosion immunity of low-current contacts in automatic devices], Elektricheskiye Kontakty [Transactions of Conference], Gosenergoizdat, 1958.

February 4, 1960.

